Charge and spin distributions in GaMnAs/GaAs Ferromagnetic Multilayers

S. C. P. Rodrigues, L. M. R. Scolfaro, J. R. Leite and I. C. da Cunha Lima*

Instituto de Física, Universidade de São Paulo,

CP 66318, 05315-970, São Paulo, SP, Brazil

G. M. Sipahi

Instituto de Física de São Carlos, Universidade de São Paulo,

CP 369, 13560-970, São Carlos, SP, Brazil

M. A. Boselli

Departamento de Física, Universidade Federal de Ouro Preto

Campus Universitrio Morro do Cruzeiro,

35.400-000 Ouro Preto, M.G., Brazil

(Dated: February 2, 2008)

Abstract

A self-consistent electronic structure calculation based on the Luttinger-Kohn model is performed on GaMnAs/GaAs multilayers. The Diluted Magnetic Semiconductor layers are assumed to be metallic and ferromagnetic. The high Mn concentration (considered as 5% in our calculation) makes it possible to assume the density of magnetic moments as a continuous distribution, when treating the magnetic interaction between holes and the localized moment on the Mn^{++} sites. Our calculation shows the distribution of heavy holes and light holes in the structure. A strong spin-polarization is observed, and the charge is concentrated mostly on the GaMnAs layers, due to heavy and light holes with their total angular momentum aligned anti-parallel to the average magnetization. The charge and spin distributions are analyzed in terms of their dependence on the number of multilayers, the widths of the GaMnAs and GaAs layers, and the width of lateral GaAs layers at the borders of the structure.

PACS numbers: 73.21.-b, 75.75.+a, 85.75.-d,72.25.Dc

I. INTRODUCTION

Recent advances on the physics and technology of GaAs-based nanostructures with diluted magnetic semiconductors (DMS) open a wide range of potential applications of these systems in integrated magneto-optoelectronic devices.[1] In $Ga_{1-x}Mn_xAs$ alloys substitutional Mn acts as an acceptor (it binds one hole), and at the same time it carries a localized magnetic moment, due to its five electrons in the 3 d shell. For x near 0.05, the alloy is a metallic ferromagnet,[2] the Curie-Weiss temperature after annealing is 160K,[3] and the free hole concentration is near $10^{20-21}cm^{-3}$. The possibility of application in Spintronics and Photonics exists because such a layer provides the injection of spin-polarized carriers in an otherwise non-magnetic semiconductor region of the device, eliminating the needs of a strong external magnetic field. Obviously, the higher the transition temperature obtained for a DMS thin layer, the higher the possibilities for a device with such a layer to operate near room temperatures. The ferromagnetic order in the metallic phase is understood, at present, as resulting from the indirect exchange between the Mn^{2+} ions due to the local spin polarization of the hole gas. This explanation implies the spin coherence length to be larger than the average distance of the localized moments. Although most of the scientific theoretical effort in this problem has been directed to understand the origin of the ferromagnetism, there are still fundamental issues to be considered in the electronic structure. For instance, the role played by the light holes and holes of the split-off band is a point yet to be understood. Such a nomenclature in GaAs is specific for bulk systems, where the tetragonal symmetry is preserved. In the case of heterostructures, where such symmetry is broken by the presence of the interfaces, a mixing occurs in the composition of the hole states. Differently from heavy holes, light hole states are not spin-eigenstates. In consequence, the occurrence of a local magnetic field is also a factor that contributes to the mixing in the composition of the hole states. This can be seen easily in the framework of the effective mass approximation and Luttinger-Kohn (LK) $\mathbf{k}\cdot\mathbf{p}$ expansion,[4] because off-diagonal terms appear in the Hamiltonian, breaking the tetragonal symmetry. Therefore, the presence of interfaces, together with a local magnetic field, claims for a better treatment of the calculation of the electronic properties in DMS heterostructures.

To the present, the six bands $\mathbf{k}\cdot\mathbf{p}$ method has been used to obtain the valence band structure of (Ga,Mn)As only in bulk systems.[5,6,7,8] Some calculations included the ef-

fects of biaxial strain, spin-orbit coupling, and exchange correlation in a parabolic band approximation.[9,10,11] In the case of quantum wells, (Ga,Mn)As multilayers and superlattices, a self-consistent calculation has been performed for parabolic heavy holes subbands.[13] Self-consistent calculations have also been performed in Refs. 10 and 11 assuming isotropic effective masses. To the exception of Ref. 12, where a Monte Carlo simulation is used, the electronic structure calculation assumes a homogeneous density of magnetic moment, as well as homogeneous negative charge concentration (due to the ionized Mn atoms). Relaxing this approximation implies in considering a multiple-scattering treatment, what is outside the scope of the present work. The homogeneous approximation for the density of magnetic and Coulomb scattering centers (localized magnetic moments and ionized impurities) provides important information concerning the carriers charge and spin distributions.

Here we present a self-consistent LK $\mathbf{k}\cdot\mathbf{p}$ calculation for GaMnAs/GaAs multilayers and superlattices. As described below, we adopt a super-cell calculation which is an extension of the LK method to treat the cases of quantum wells and superlattices (SL). The structure we consider consists of substitutional Mn ions uniformly distributed in $Ga_{0.95}Mn_{0.05}As$ layers of width d_1, with a hole concentration equivalent, in bulk, to 1x10^{20} cm^{-3}, assumed to be metallic and ferromagnetic, at T=0K. The DMS are separated by non-magnetic GaAs layers of width d_2. Before the first DMS layer and after the last one, GaAs lateral layers of width s complete the structure, as shown in Fig. 1. The super-cell model consists of placing this "active part", described so far, between thick layers of a large gap material, assumed here to be AlAs, and treating the whole system as a superlattice.

The final spin and charge configuration contains a complete information about the composition of heavy holes and light holes in the structure. Carriers are anti-parallel heavy holes, and anti-parallel light holes, in a lesser amount. A strong spin polarization is observed, and the charge is concentrated mostly on the GaMnAs layers. The charge and spin distributions are analyzed in terms of their dependence on the number of multilayers, the widths d_1 and d_2, as well as the widths of the lateral GaAs layers.

II. MAGNETIC INTERACTION IN THE CONFINED LK MODEL

The interaction between free holes and the localized magnetic moments is well described by the Kondo-like term

$$V_{mag}(\mathbf{r}) = -I \sum_i \vec{s}(\mathbf{r}) \cdot \mathbf{S}(\mathbf{R}_i)\delta(\vec{r} - \mathbf{R}_i), \tag{1}$$

where I is the $sp-d$ interaction. The localized spin of the Mn ion $\vec{S}_i$ at position $\vec{R}_i$ is treated as a classical variable, since it results of the five $3d$ electrons obeying Hund's rule, and no hybridization with carriers is considered, due to the high difference in energies. $\vec{s}(\vec{r})$ is the spin operator of the carrier at position $\vec{r}$. At zero temperature, assuming a complete alignment of the localized magnetic moment, i.e., $\mathbf{S}(\mathbf{R}_i) = \mathbf{S}$, we have:

$$V_{mag}(\vec{r}) = -I\mathbf{S} \cdot \vec{s}(\vec{r}) \sum_i \delta(\vec{r} - \mathbf{R}_i) = -\frac{I}{2}\mathbf{S} \cdot \vec{\sigma}\rho_i(\vec{r}). \tag{2}$$

In the last expression we used $\vec{\sigma} = \hat{i}\sigma_x + \hat{j}\sigma_y + \hat{k}\sigma_x z$ to denote the three Pauli matrices; $\rho_i(\vec{r})$ is the density of magnetic impurities. Assuming a homogeneous distribution of the localized magnetic dipoles inside the DMS layers , we have $\rho_i(\vec{r}) \approx xN_0 g(z)$, where N_0 is the the density of cations, x is the substitutional concentration of Mn, and $g(z) = 1$ if z lies inside a DMS layer, $g(z) = 0$ otherwise. In that case the magnetic interaction becomes:

$$V_{mag}(z) = -\frac{x}{2}N_0\beta g(z)\vec{M} \cdot \vec{\sigma}. \tag{3}$$

In Eq.(3) we have explicitly taken into consideration that carriers are holes, replacing I by β. For GaMnAs, $N_0\beta = -1.2$ eV.[14] For electrons, $N_0\alpha = 0.2$ eV.[15] Were the spin of the particles well defined, this term would represent, in bulk, a shift on the top (bottom) of the valence (conduction) band. This is not the case, as discussed above, for light holes and split-off holes in GaAs.

It is well known that the valence bands in GaAs at the Γ point split, due to spin-orbit interaction, into four $j = 3/2$ states belonging to the Γ_8 representation, and two $j = 1/2$ states belonging to the Γ_7 representation. These two are separated from the Γ_8 states by the spin-orbit energy Δ, which is 340 meV in GaAs.[16] We adopt the notation $\mid j, m_j >$ to represent the Γ_8 and the Γ_7 states, making use of the fact that these states are also eigenstates of the total angular momentum operator $\mathbf{J} = \mathbf{L} + \vec{s}$, with eigenvalue j, and simultaneously eigenstates of its z-component, J_z, corresponding to the eigenvalue m_j. Notice that the

Γ_8 states $\mid v1 >$ and $\mid v2 >$ both having $j = 3/2$ but with $m_j = 3/2$ and $m_j = -3/2$, respectively, are called heavy holes states, having their spins well defined, being "up", i.e., aligned with $\mathbf{J}$, and "down", anti-aligned. They can be represented by using as a basis the three p-type states in the directions x, y, and z:[17]

$$\mid v1 > \; = \; \mid \frac{3}{2}\frac{3}{2} >= \frac{1}{\sqrt{2}}(\mid x + iy \uparrow >) \tag{4}$$

$$\mid v2 > \; = \; \mid \frac{3}{2}\frac{\bar{3}}{2} >= \frac{i}{\sqrt{2}}(\mid x - iy \downarrow >) \tag{5}$$

The other states, the light hole states $\mid v3 >$ and $\mid v4 >$ corresponding also to $j = 3/2$, but with $m_j = 1/2$ and $m_j = -1/2$, and the split-off states $\mid v5 >$ and $\mid v6 >$ corresponding to $j = 1/2$ with $m_j = 1/2$ and $m_j = -1/2$, do not have well defined spins:

$$\mid v3 > \; = \; \mid \frac{3}{2}\frac{1}{2} >= \frac{i}{\sqrt{6}}(-2 \mid z \uparrow > + \mid x + iy \downarrow >) \tag{6}$$

$$\mid v4 > \; = \; \mid \frac{3}{2}\frac{\bar{1}}{2} >= \frac{1}{\sqrt{6}}(\mid x - iy \uparrow > +2 \mid z \downarrow >) \tag{7}$$

$$\mid v5 > \; = \; \mid \frac{1}{2}\frac{1}{2} >= \frac{1}{\sqrt{3}}(\mid z \uparrow > + \mid x + iy \downarrow >) \tag{8}$$

$$\mid v6 > \; = \; \mid \frac{1}{2}\frac{\bar{1}}{2} >= \frac{i}{\sqrt{3}}(- \mid x - iy \uparrow > + \mid z \downarrow >) \tag{9}$$

The kinetic, Hartree, and the exchange-correlation terms appear in this formalism as the well known components of the LK matrix.[4] In multilayers and superlattices the mismatches of the valence and conduction bands, which play the roles of confining potentials, are to be added. Differences on the lattice parameters introduce the additional terms of the strain. Here we have also to introduce the magnetic potential given by Eq.(3). Two distinct cases may be considered, since a break in the $\mathrm{T_d}$ symmetry occurs: magnetization "in-plane" (occurring parallel to the interfaces) $\mathbf{M}_{\parallel} = M_x\hat{i} + M_y\hat{j}$, and "perpendicular to the plane", $\mathbf{M}_{\perp} = M_z\hat{k}$. The latter is assumed to be in the growth direction, here considered as the z-axis. Notice that in the presence of a confining potential created by the interfaces, $V_c(z)$, the operators $\hat{J}_x$ and $\hat{J}_y$ no more commute with the LK Hamiltonian. In bulk, however, within the homogeneous magnetization approach, there is no distinction between these two cases. Once we are not trying to explain the origin of the ferromagnetic order in these systems, the occurrence of the magnetization being "in plane" or "perpendicular-to-the-plane" is assumed to be provided by an external weak magnetic field, which does not interfere on the electronic structure, directly.

For the sake of obtaining the LK matrix for heterostructures, it is necessary to calculate first the matrix elements $< j, m|V_{mag}|j', m' >$ for each constituent DMS layer, in bulk. This is easily done by observing that

$$\mathbf{M}_{\perp} \cdot \vec{\sigma}| \uparrow> \; = \; M_z| \uparrow>, \tag{10}$$

$$\mathbf{M}_{\perp} \cdot \vec{\sigma}| \downarrow> \; = \; -M_z| \downarrow>, \tag{11}$$

and

$$\mathbf{M}_{\parallel} \cdot \vec{\sigma}| \uparrow> \; = \; (M_x + iM_y)| \downarrow> \equiv M_+| \downarrow>, \tag{12}$$

$$\mathbf{M}_{\parallel} \cdot \vec{\sigma}| \downarrow> \; = \; (M_x - iM_y)| \uparrow> \equiv M_-| \uparrow>, \tag{13}$$

Making use of the approximation given in Eq.(3) and the results in Eqs. (10-13), we have for the LK matrix of V_{mag} at the Γ point:

$$\tilde{V}_{mag} = -\frac{x}{6} N_0 \beta \begin{pmatrix} 3M_z & 0 & i\sqrt{3}M_- & 0 & \sqrt{6}M_- & 0 \\ 0 & -3M_z & 0 & -i\sqrt{3}M_+ & 0 & -\sqrt{6}M_+ \\ -i\sqrt{3}M_+ & 0 & M_z & 2iM_- & 2\sqrt{2}iM_z & -\sqrt{2}M_- \\ 0 & i\sqrt{3}M_- & -2iM_+ & -M_z & \sqrt{2}M_+ & -2\sqrt{2}iM_z \\ \sqrt{6}M_+ & 0 & -2\sqrt{2}iM_z & \sqrt{2}M_- & -M_z & iM_- \\ 0 & -\sqrt{6}M_- & -\sqrt{2}M_+ & 2\sqrt{2}iM_z & -iM_+ & M_z \end{pmatrix} \tag{14}$$

During the last years the LK model has been adapted to quantum wells and superlattices (SL), as described in Refs. 17,18,19. We adopt that approach, using a super-cell model. This means that we consider an unit cell consisting of the active region plus a thick insulator layer. The number of DMS layers in the unit cell can be varied at will. We assume, then, an infinite SL in the [001] direction. The multiband effective-mass equation (EME) is represented with respect to plane waves with wavevectors $K = (2\pi/a)l$ (l an integer and a the SL period) equal to the reciprocal SL vectors. A detailed description of the method can be found in Ref. 22. The rows and columns of the 6×6 LK Hamiltonian relate to the Bloch-type eigenfunctions $|j, m_j, \vec{k} >$ of the Γ_8 heavy-hole bands, and the Γ_7 spin-orbit-hole band; $\vec{k}$ denotes a vector of the first Brillouin zone. Expanding the EME with respect to plane waves $< z \mid K >$ means representing this equation in terms of the Bloch functions $< \mathbf{x} \mid j, m_j, \vec{k} + K\mathbf{e}_z >$. For a Bloch function $< z \mid E, \vec{k} >$ of the SL corresponding to energy E and wavevector $\vec{k}$,

the EME takes the form:

$$\sum_{j',m'_j,K'} < j, m_j, \vec{k}, K \mid T + H_S + V_{het} + V_C + V_{xc} + V_{mag} \mid j', m'_j, \vec{k}, K' > \times$$
$$< j', m'_j, \vec{k}, K' \mid E, \vec{k} >= E(\vec{k}) < j, m_j, \vec{k}, K \mid E, \vec{k} >, \qquad (15)$$

where T is the unperturbed kinetic energy term generalized for a heterostructure,[20] H_S is the strain energy term originating from the lattice mismatch, V_{het} is the square potential due to the difference between energy gaps, V_{xc} is the exchange-correlation potential, and V_C is the sum of the Hartree potential with the ionized acceptor potential. Finally, V_{mag} is given by Eq.(3), for each material. The Luttinger parameters and the other terms appearing in the secular equation are to be taken for each epitaxial layer of the SL.[21] For instance, in the case of the magnetic interaction we have:

$$< j, m, \vec{k}, K|V_{mag}|j', m', \vec{k}', K' >=< \vec{k}, K|\tilde{V}_{mag}^{jm;j'm'} g(K' - K)|\vec{k}', K' >, \qquad (16)$$

where the integral

$$g(K' - K) = \frac{1}{d}\int_0^d e^{-iKz} g(z) e^{iK'z} \qquad (17)$$

is performed in a DMS layer of width d.

The self-consistent potentials and the charge densities are obtained by solving the multi-band EME equation and the Poisson equation:

$$< j, m_j, \vec{k}, K \mid V_C \mid j', m'_j, \vec{k}, K' >= \frac{4\pi e^2}{\kappa} \frac{1}{|K - K'|^2} < K \mid \rho^+ + \rho^- \mid K' > \delta_{j,j'}\delta_{m_j,m'_j}, \quad (18)$$

where κ is the dielectric constant of the host, and ρ^+ and ρ^- are the density of charge of holes and acceptors, respectively, expressed in plane-wave representation.

III. RESULTS

The DMS layers work effectively as barriers or wells for spins parallel (up) and antiparallel (down) to the local average magnetization, depending on the sign of $N_0\beta$ for valence band, and $N_0\alpha$ for conduction band. These DMS layers are assumed to be ferromagnetic and metallic, with a 3-D equivalent hole density p = 1 x 10^{20} cm^{-3}, a substitutional Mn concentration of 5%, at temperature T= 0 K, and an average magnetization $\langle M \rangle$=5/2.

In Fig. 2 we present (a) the valence band structure (hole binding energy) and (b) potential profiles for a system consisting of six DMS layers, with d_1=20 Å and d_2=30 Å. Energies are

reckoned from the top of the Coulomb barrier, as in Ref. 22. The magnetization is assumed to be in the z-direction. The subbands are hybrid states, since they are a mixing of all kinds of holes. However, at the Γ-point the lowest lying states have a dominant component. For instance, the first three states are almost entirely heavy holes "down". The mixing becomes stronger in the more excited states, and as we go out of the Γ-point. In Fig. 2 we named the band by its dominant component at the Γ-point. Here, "up" and "down" refer to the sign of m_j, the z-component of the total angular momentum. In other words, "up" means parallel to the average magnetization, while "down" means anti-parallel. The Γ-Δ (Γ-Z)-line corresponds to wave vectors $\vec{k}$ perpendicular (parallel) to the SL axis. The Fermi energy is also indicated. Strong non-parabolicity arises in the subbands along the (Γ-Δ)-line, which leads to remarkable anti-crossing behavior. We also observe that several levels are occupied, most of them are heavy and light hole down. It is possible to understand this behavior by observing Fig. 2(b), which shows the self-consistent hole band potential profile for each carrier. The confinement for heavy and light holes down are deeper than the cases where the z-components of the total angular momentum are up.

Fig. 3 shows the carriers distribution for the structure with six DMS layers described in Fig. 2. The results are shown for lateral GaAs layers of width s =0, 10, 20, 30, 40, 50 and 60 Å. We notice that, except for the heavy hole with $m_j = 3/2$ (up), carriers concentrate on the DMS layers. The heavy holes up concentrate in the non-magnetic region as a consequence of the strong magnetic repulsion. After $s = 50$Å the carriers distribution becomes independent of the lateral GaAs widths.

Fig. 4 shows the carriers density for active regions consisting of 1 to 9 DMS layers. We fixed d_1=20 Å and d_2=30 Å. The charge density is plotted for each component. As before, "up" and "down" refer to the sign of the m_j component of the total angular momentum. These results are consistent with the electronic structure shown in Fig. 2, since the lowest levels are mostly heavy and light holes down. Observe that in all multilayered structures (2 to 9 DMS layers) the charge is concentrated almost entirely inside the DMS layers. Again, the exception is the heavy hole up component, whose density is higher in the non-magnetic regions for the reasons explained above.

Up to now the distribution of charge in the multilayered structure has been shown in terms of carriers total angular momentum components. For the sake of completeness, it is also interesting to know how the charge is distributed in terms of the spin polarization. This

can be easily obtained, since the light holes are mixed states of up and down spins with defined probabilities. The results for these multilayers are shown in Fig.5 in terms of the spin components of the charge density. There is a strong spin polarization, dominated by heavy and light holes down spins.

In Fig. 6 we analyze the dependence of the effective two-dimensional hole concentration, N_{2D}, which is the integrated 3-D density on the z-direction for each component. The DMS layers widths are changed, while keeping fixed the width of the GaAs layers, d_2=30 Å. The calculation is performed for 6 DMS layers. For the heavy and light hole down, the 2-D densities are much higher then those associated to positive values of m_j. The difference is one order of magnitude, in the case of heavy holes, due to its higher effective mass and profile potential that provide a higher occupation inside the DMS layers.

Finally, in Fig. 7 we show N_{2D} as a function of the non-magnetic layer width, d_2, with d_1=20 Å, for each carrier, heavy and light hole (down and up). The calculation is performed for 4, 5, 6 and 7 DMS layers.

IV. CONCLUSIONS

In summary, we have investigated the electronic structure of $Ga_{0.95}Mn_{0.05}As$/GaAs multilayers by using a super-cell model in the framework of the Luttinger-Kohn **k.p** approximation. The unit in the super-cell is a AlAs/n($Ga_{0.95}Mn_{0.05}As$/GaAs)/AlAs structure, with n being the number of DMS layers, grown in the [100] direction. The DMS layers are assumed to be metallic and ferromagnetic, at T=0K. A small magnetic field is applied in the growth direction to guarantee the magnetization to be perpendicular to the plane, but it does not affect the electronic structure. Several subbands are occupied. They are mostly heavy holes with $m_j = -3/2$, the carrier density being higher in the DMS layers. However, a non-negligible part of carriers are light holes with $m_j = -1/2$, also concentrated on the same region as the heavy holes. Actually, what is observed is the appearance of two different channels, one with the z-component of the total angular momentum aligned with the average magnetization, which is highly concentrated on the DMS layers, and another, with opposite orientation whose distribution is more concentrated on the non-magnetic layers of the active region, the latter channel being much less dense. These results are in qualitative agreement with those obtained in Ref. 23 showing the electronic structure calculations

in digital ferromagnetic heterostructures of GaAs/(Ga,Mn)As and AlAs/(Ga,Mn)As/GaAs using density-functional theory in the local spin-density approximation. As a consequence of both magnetic and Coulomb interactions - here included the hole-hole interaction - the spin-polarized charge tends to be slightly non-periodically distributed as the number of DMS layers increases. Carriers polarized anti-parallel to the magnetization tend to concentrate a little more at the borders of the structure, while carriers polarized in the opposite direction tend to concentrate on the middle.

From the point of view of the observation of a ferromagnetic multilayer with a high transition temperature (we recall that we have assumed in our calculation T=0K), it is interesting to have a strong "spin-polarized" charge density in the DMS layers, while keeping some charge in between to guarantee the inter-layer interaction.[24,25] However, for obtaining a high mobility spin-polarized current, a structure should be grown in which the in-plane transport is realized with spin-polarized carriers concentrated in a region of high mobility, away from the scatterers. Therefore, the ideal distribution of charge and spin depends on the purpose of the structure. The results we have obtained points to the possibility of engineering the spin-polarized charge distribution by the right choice of the magnetic layers and the band mismatches with the non-magnetic spacers.

Acknowledgments: Work supported by CNPq (NanoSemiMat network), and FAPESP. ICCL thanks the LNMS group for its generous hospitality.

---

* On leave from Instituto de Física, Universidade do Estado do Rio de Janeiro, Rio de Janeiro, R.J., Brazil

[1] Y. Ohno, D.K. Young, B. Beschoten, F. Matsukura, H. Ohno and D.D. Awschalom, Nature **402**, 790 (1999); T. Dietl, H. Ohno, F. Matsukura, J. Cibert, and D. Ferrand, Science **287**, 1019 (2000); see also the special issue of Semicond. Sci. Technol. **17** (2002).

[2] F. Matsukura, H. Ohno, A. Shen, and Y. Sugawara, Phys. Rev. B **57**, R2037 (1998).

[3] D. Chiba, K. Takamura, F. Matsukura, and H. Ohno, Appl. Phys. Lett. **82**, 3020 (2003).

[4] J. M. Luttinger and W. Kohn, Phys. Rev. **97**, 869 (1955).

[5] T. Dietl, H. Ohno, and F. Matsukura, Phys. Rev. B **63**, 195205 (2001); T. Dietl *et al*, Physica E **7**, 967 (2000).

[6] B. Lee, T. Jungwirth, and A. H. MacDonald, Phys. Rev. B **61**, 15606 (2000).

[7] I. Vurgaftman and J. R. Meyer, Phys. Rev. B **64**, 245207 (2001).

[8] M. Abolfath, T. Jungwirth, A. H. MacDonald, Physica E **10**, 161 (2001).

[9] T. Dietl, Semic. Sc. Technol. **17**, 377 (2002).

[10] H. J. Kim, K. S. Yi, N. M. Kim, S. J. Lee, J. J. Quinn, Physica E **12**, 383 (2002).

[11] J. Jungwirth, B. H. Lee, and A. H. MacDonald, Physica E **10**, 153 (2001).

[12] John Schliemann, Jürgen König, and A. H. MacDonald, Phys. Rev. B **64**, 165201 (2001).

[13] L. Loureiro da Silva, M. A. Boselli, I. C. da Cunha Lima, X. F. Wang, and A. Ghazali, Appl. Phys. Lett. **79** 3305 (2001).

[14] J. Okabayashi, A. Kimura, O. Rader, T. Mizokawa, A. Fujimori, T. Hayashi, and M. Tanaka, Phys. Rev. B **58**, R4211 (1998).

[15] J. Szczytko, W. Mac, A. Twardowski, F. Matsukura, and H. Ohno, Phys. Rev. B **59**, 12935 (1999).

[16] J. Wu, H. Yaguchi, K. Onabe, and Y. Shiraki, J. Cryst. Growth **197**, 73 (1999).

[17] See, for instance, R. Enderlein and N. J. Horing, *Fundamentals of Semiconductor Physics and Devices*, (World Scientific, 1997).

[18] R. Enderlein, G. M. Sipahi, L. M. R. Scolfaro and J. R. Leite, Phys. Rev. Lett. **79**, 3712 (1997); *ibid* **80**, 3160 (1998).

[19] S. C. P. Rodrigues, G. M. Sipahi, L. M. R. Scolfaro, and J. R. Leite, J. Phys.: Condens. Matter **13**, 3381 (2001).

[20] S. C. P. Rodrigues, G. M. Sipahi, L. M. R. Scolfaro, and J. R. Leite, Appl. Phys. Lett. **76**, 1015 (2000).

[21] T. P. Pearsall, Strained-Layer Superlattices : Physics, vol 32 Semiconductor and Semimetals (Academic Press 1990).

[22] S. C. P. Rodrigues, G. M. Sipahi, L. M. Scolfaro, and J. R. Leite, J. Phys.: Condens. Matter **14**, 5813 (2002).

[23] Stefano Sanvito, Phys. Rev. B **68**, 054425 (2003).

[24] M. A. Boselli, I. C. da Cunha Lima, and A. Ghazali, Phys. Rev. B **68**, 085319 (2003).

[25] M. A. Boselli, I. C. da Cunha Lima, A. Troper, J. R. Leite, and A. Ghazali, Appl. Phys. Lett. **84**, 1138 (2004).

FIG. 1: The model structure: the DMS layers of width $d1$ are separated by non-magnetic GaAs layers of width d_2. At the left of the first DMS layer and at the right of the last one, GaAs lateral layers of width s complete the "active" parts. The "active" parts are separated, themselves, by thick AlAs barriers.

FIG. 2: (a)Valence band structures for GaAs/GaAs:Mn multiple QWs along high symmetry lines Γ-Z and Γ-Δ, with $d_1 = 20$ Å and $d_2 = 30$ Å. We named the band by its dominant component at the Γ-point. Solid lines correspond to subbands which, at the Γ-point, are mostly heavy holes down, dashed lines to light hole down, dotted lines to heavy hole up, and dotted-dashed lines to light holes up. The Fermi energy is also indicated (short-dashed line). (b) the corresponding potential profile for each carrier, down and up. Energies are reckoned from the top of the Coulomb barrier.

FIG. 4: Particle density of heavy and light holes for a structure consisting from 1 to 9 DMS layers. Widths d_1 and d_2 as in Fig.1.

FIG. 5: Same as in Fig. 3, for each carrier spin component.

FIG. 6: N_{2D} as a function of the DMS layer width d_1. The width of the non-magnetic layers are fixed, $d_2 = 30$ Å.

FIG. 7: N_{2D} as a function of the non-magnetic layer width d_2, for 4, 5, 6 and 7 DMS layers. The widths of the DMS layers are fixed, $d_1 = 20$ Å.

FIG. 3: Density distribution of heavy and light holes for six DMS layers with $d_1 = 20$Å, $d_2 = 30$Å, and lateral GaAs widths $s = 0, 10, 20, 30, 40, 50$ and 60Å.

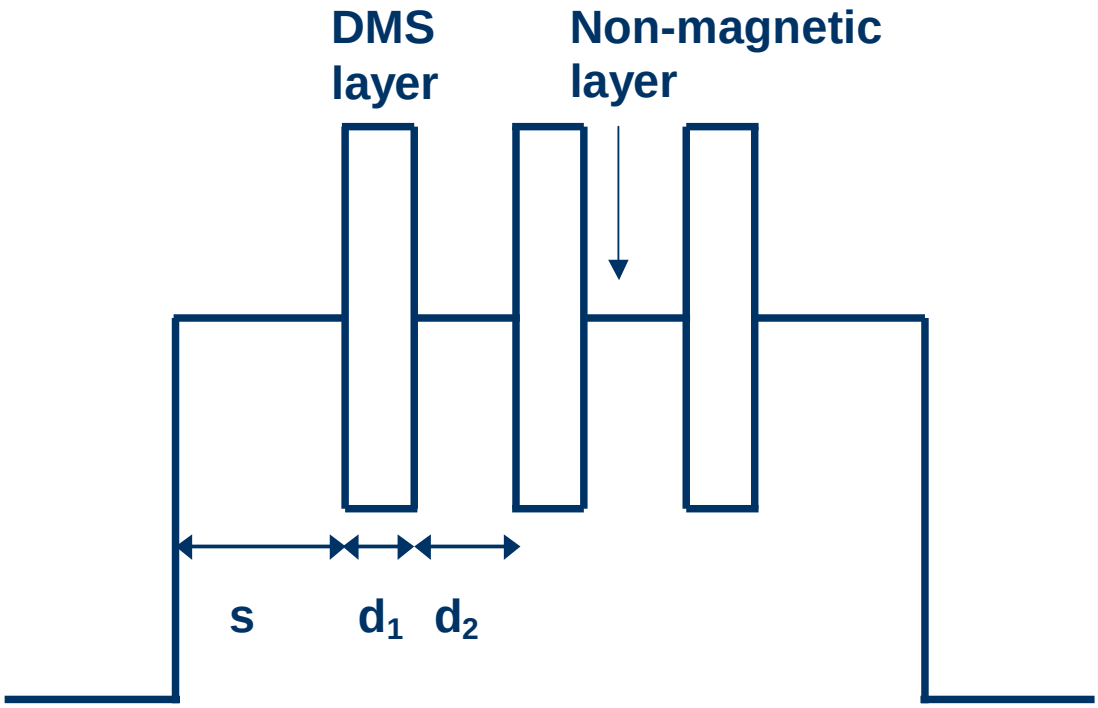
DMS
layer
Non-magnetic
layer
s
d_1
d_2

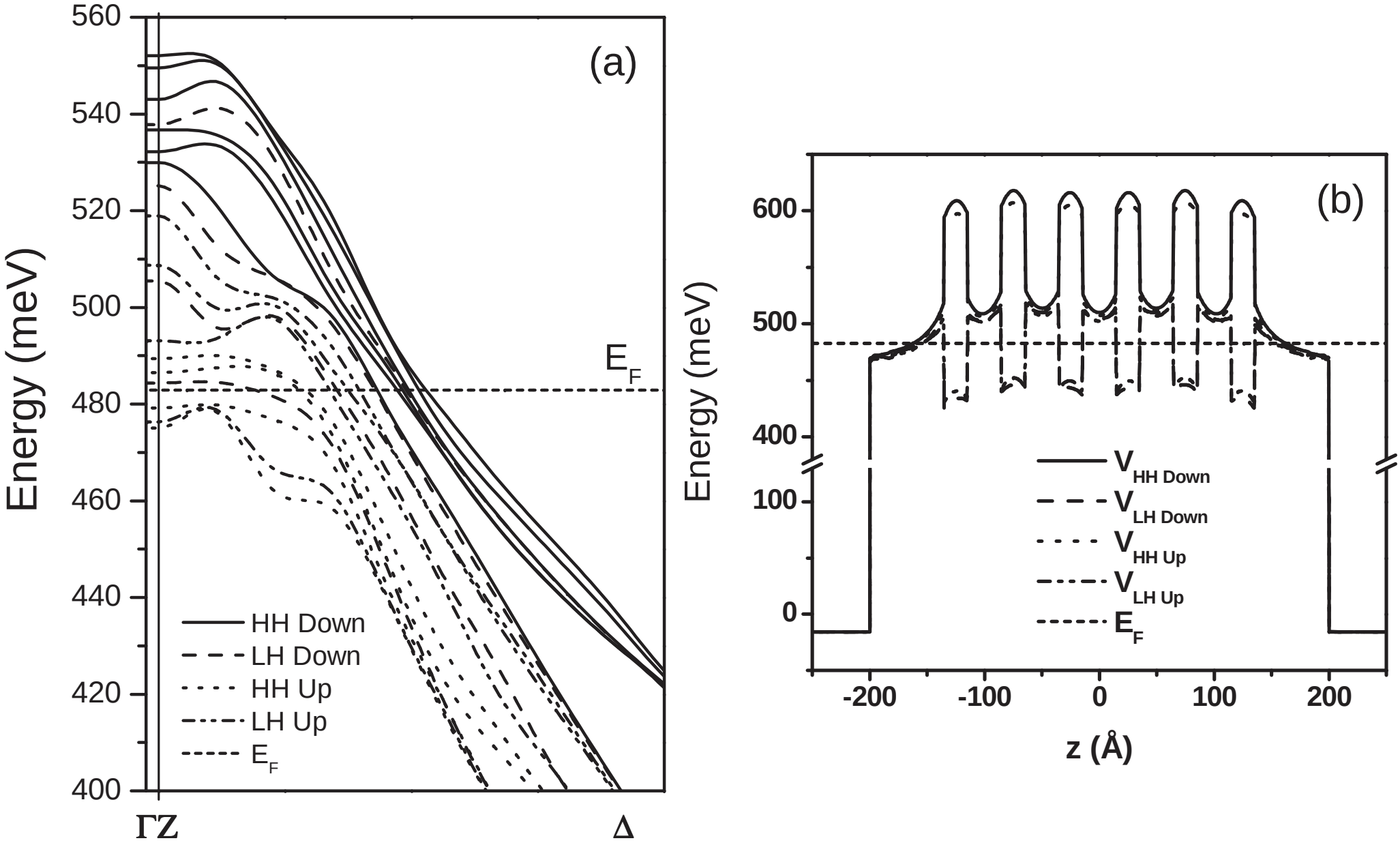
(a)
Energy (meV)
560
540
520
500
480
460
440
420
400
E_F
HH Down
LH Down
HH Up
LH Up
E_F
ΓZ
Δ
(b)
Energy (meV)
600
500
400
100
0
$V_{HH\ Down}$
$V_{LH\ Down}$
$V_{HH\ Up}$
$V_{LH\ Up}$
E_F
-200
-100
0
100
200
z (Å)

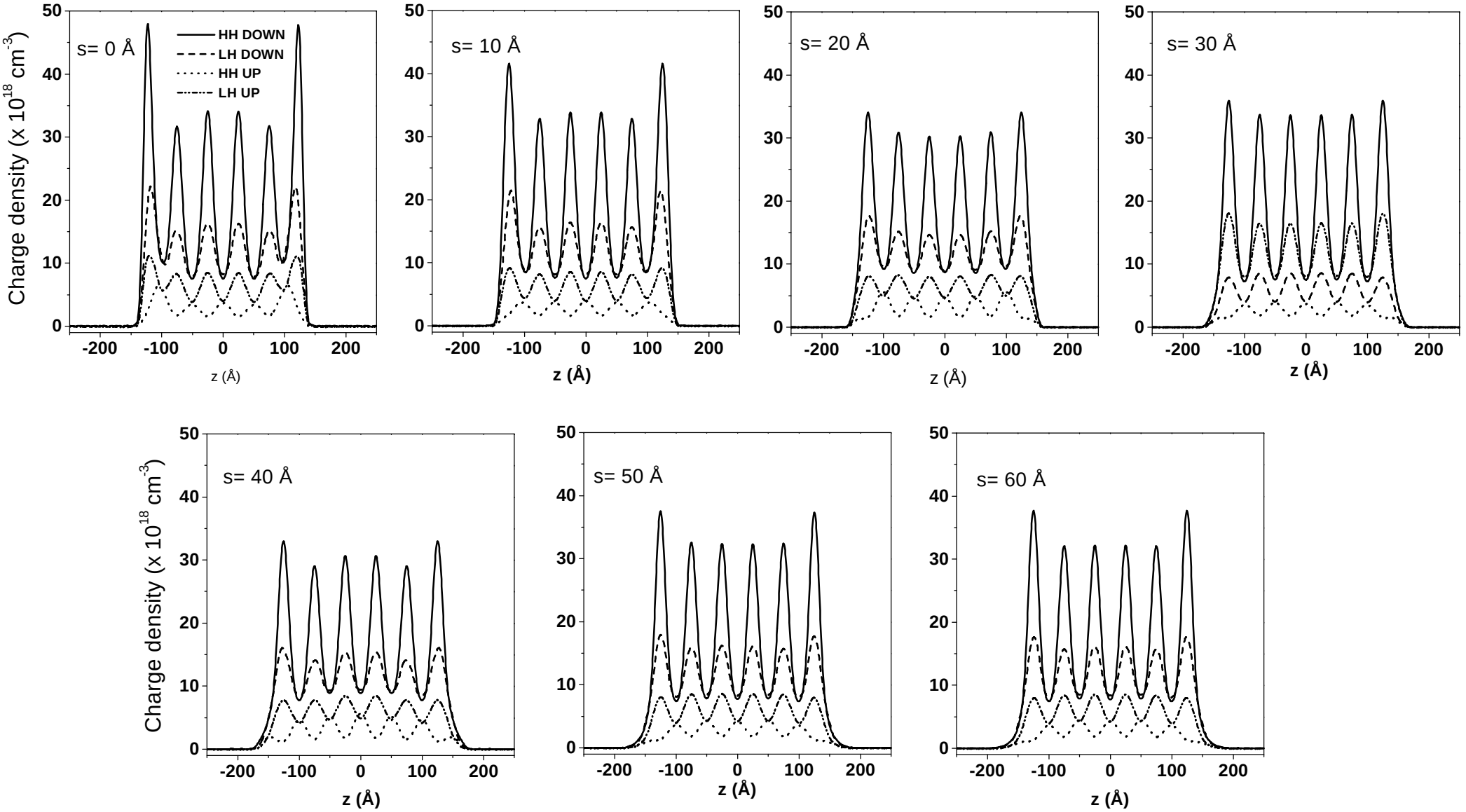
s= 0 Å
HH DOWN
LH DOWN
HH UP
LH UP
Charge density (x 10^18 cm^-3)
z (Å)
s= 10 Å
s= 20 Å
s= 30 Å
s= 40 Å
s= 50 Å
s= 60 Å

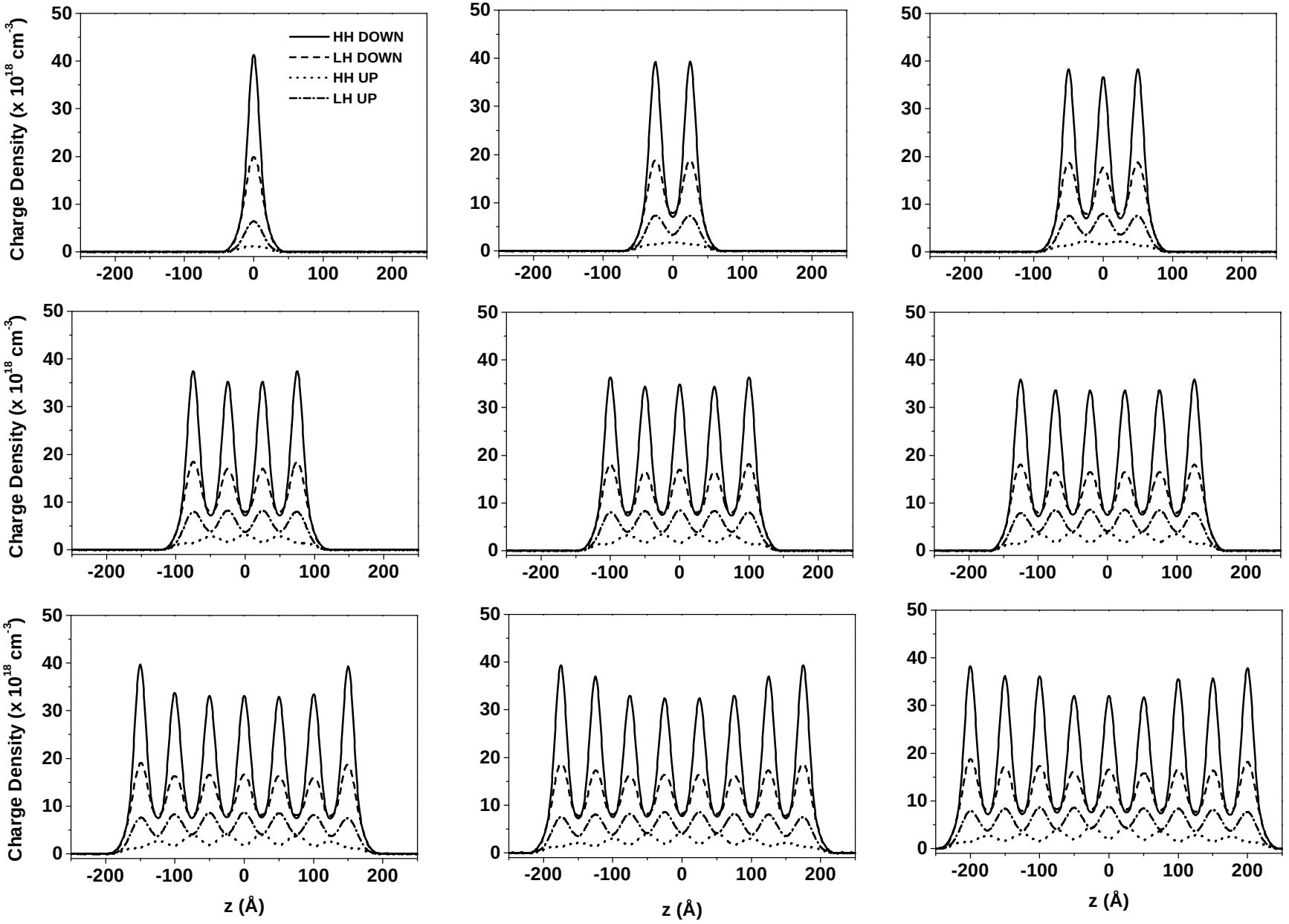
HH DOWN
LH DOWN
HH UP
LH UP
Charge Density (x 10^18 cm^-3)
z (Å)

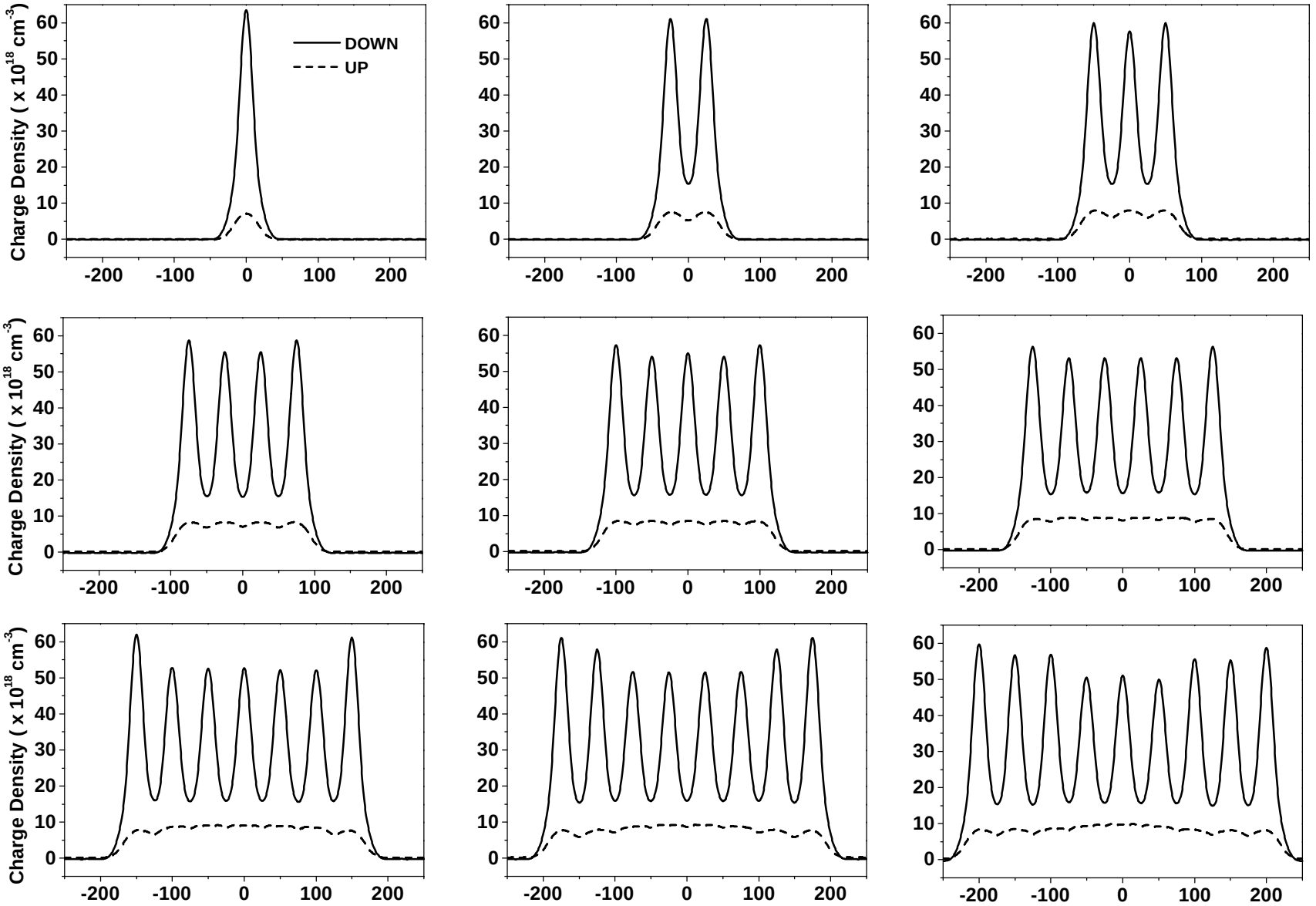
DOWN
UP
Charge Density (x 10^18 cm^-3)
0
10
20
30
40
50
60
-200
-100
0
100
200

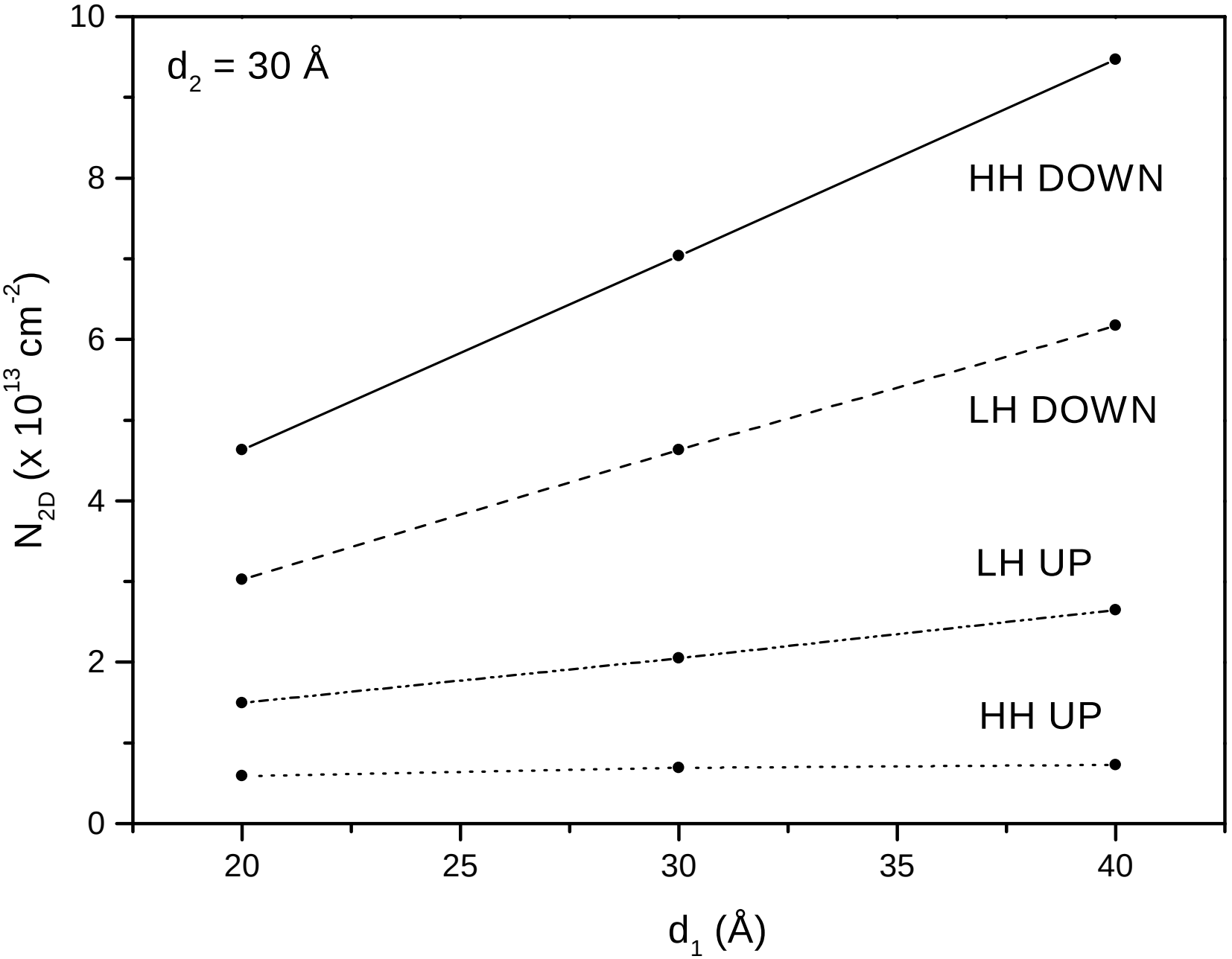
d2 = 30 Å
HH DOWN
LH DOWN
LH UP
HH UP
N2D (x 10^13 cm^-2)
d1 (Å)
0
2
4
6
8
10
20
25
30
35
40

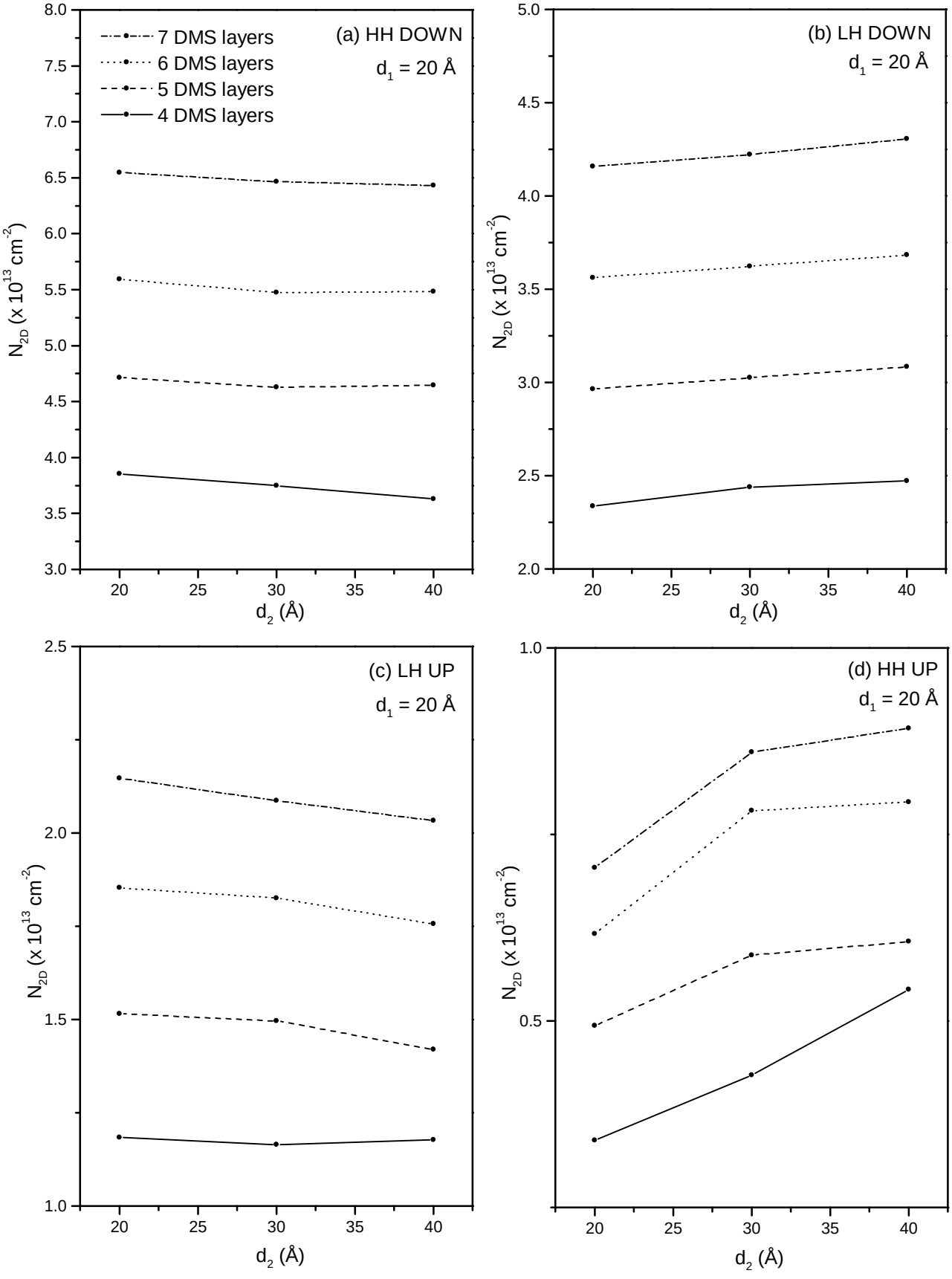
7 DMS layers
6 DMS layers
5 DMS layers
4 DMS layers
(a) HH DOWN
d1 = 20 Å
(b) LH DOWN
d1 = 20 Å
(c) LH UP
d1 = 20 Å
(d) HH UP
d1 = 20 Å
N2D (x 10^13 cm^-2)
d2 (Å)